First characterization of Gamkonora gas emission, North Maluku, East Indonesia

Ugan B. Saing[1], Philipson Bani[2], Nia Haerani[1], Alessandro Aiuppa[3], Sofyan Primulyana[1], Hilma Alfianti[1], Devy K. Syahbana[1], Kristianto[1]

[1]Center for Volcanology and Geological Hazard Mitigation, Jl. Diponegoro No 57, Bandung, Indonesia
[2]Laboratoire Magmas et Volcans, Univ. Blaise Pascale—CNRS—IRD, OPGC, 63000 Clermont-Ferrand, France
[3]Dipartimento DiSTeM, Università di Palermo, Italy

Abstract

Gamkonora is an active volcano capable of intense manifestations that regularly forced thousands of inhabitants to flee their villages. The most extreme event in 1673 was a VEI 5 eruption that enduced pich-dark ambiance over the region, whilst ash falls were reported up to south philippines, ~1000 km northwest of the volcano. Paradoxically however, only few work has been carried out on this volcano so far, and little is known about its activity. Here we present the results of the first gas measurement obtained in September 2018 using a MultiGAS instrument and a scanning UV spectrometer. Our results reveal a small but detectable magmatic gas release on Gamkonora, with daily H_2O, CO_2, SO_2, H_2S and H_2 outputs of 129 t, 13 t, 3.4 t, 1.1 t and 0.03 t respectively. Gas composition is dominated by water (H_2O/SO_2 ratio of circa 135), as typical for arc volcanos, whilst the CO_2/S_t mean ratio of 3.5 is within the compositional range for high-temperature gas emissions from other volcanoes in Indonesia. Bulk rock analyses indicate that a basaltic andesite to andesite source sustains the current activity of Gamkonora. Morphology analysis points to a possible 5 km^3 mass collapse on the southern part of the crater.

Keywords: Gamkonora volcano, magmatic degassing, gas emission budget.

1. Introduction

The Indonesian archipelago is part of the western Pacific ring of fire with 127 active volcanoes distributed along four distinct arcs, including Sunda arc, Banda arc, Maluku arc and Sulawesi-Sangihe arc (Fig. 1). Out of the above 127 volcanoes, 77 have erupted at least once since 1600. These latter volcanoes are classified as A-Type in the Indonesian volcanological community, and they are currently monitored by CVGHM (Center for Volcanology and Geological Hazard Mitigation). Unfortunately, many of these volcanoes are still poorly studied, particularly those located to the eastern part of the archipelago. This is the case of Gamkonora (Fig. 1), one of the least accessible volcanoes in Indonesia, for which very little is known about its present and past activity. This is a paradox considering that Gamakonora has experienced intrs recent past one of the few hystorical VEI 5 type (plinian) eruption in the area (Siebert et al., 2010). This cataclysmic VEI 5 eruption of Gamkonora occurred on May 20, 1673 (GVP,

1981) and, although litlle studied, is known from hystorical reports to have caused pich-dark ambiance on Ternate, a big and flourish city in the 15-17 centuries, situated 70 km southwest of the volcano. Manado and Sangir Islands located ~300 km west and northwest of the volcano were also affected by heavy ash fall. The region of Mindanao (southern Philippines) which is ~1000 km northwest of the volcano also witnessed ash fall (Kusumadinata, 1969; Data dasar, 2011; GVP, 2013). The dead toll behind this eruption is unknown but it is suspected to be high (Kusumadinata, 1969; Data dasar, 2011). The eruption has extensively devasted the forest and agricultural surfaces on the northeast Halmahera Island with consequences over several months. It has also been proposed that a tsunami event occurred in 1673, triggered by an earthquake and landslide at Gamkonora, which nundated nearby villages along the coast (e.g., Paris et al., 2014). Hitherto the connection with the VEI 5 eruptive was not clearly explicited. In the more recent history of Gamkonora, only VEI 1-2 eruptions are reported (Table 1). Some of these events have ejected incandescent material above the summit leading to forest fires in 1926, whilst in 1981 an eruption forced 3500 inhabitants to leave their villages. During the 2007 eruption, have 8400 inhabitants were evacuated by authorities (Table 1).

In 2018, the local observatory recorded increasing seismicity, which was interpreted as caused by shallow degassing activity rather than by other eismicity mechanisms (such deep volcano-tectonic events or harmonic tremor) (REF). We therefore conducted field observations at the summit of Gamkonora on September 24, 2018 (this work) which, although revealing mild (un-pressurized) gas emissions, allowed for the first time to characterize the gas composition and emission budget for the volcano. Here we report on these gas results, and we also aim to provide further details on the summit moprhology of the volcano, on the surface thermal energy release inside the summit crater, and on its shallow degassing dynamics.

2. Methodology

To measure the gas composition at Gamkonora, we used a portable version of the Palermo-type Multi-GAS (Aiuppa et al., 2012) that measures the concentrations of CO_2, SO_2, H_2S, H_2 as well as pressure (P), temperature (T) and relative humidity (RH). This latter is then converted into H_2O concentration in the plume following Buck (1981):

$$H_2O = 6.1121*(1.0007+3.46*P^{-6})*\exp((17.502*T)/240.97+T)*RH*10^{4}*P^{-1}$$

CO_2 gas is detected by near dispersive infra-red spectroscopy (Gascard, range of 0-3,000 ppm), while SO_2, H_2S and H_2 gases are detected by specific electrochemical sensors (models 3ST/F, EZ3H, and EZT3HYT "Easy Cal" respectively, all from City Technology, with a calibration range of 0-200 ppm). The system is powered by a small internal LiPo battery (6 Ah 12 V) and collects data at 0.5 Hz rate. On Gamkonora, the MultiGAS was positioned at the edge of the crater in the plume (Fig. 2) and continuously recorded for 2.5 h. The raw data were stored in the data logger and then processed and analyzed using the Ratiocalc software (Tamburello, 2015). Uncertainties in derived gas ratios are estimated at ≤10%, except for H_2O/SO_2 (≤30%). SO_2 flux measurements were achieved using a Ocean Optics USB2000+

spectrometer with a spectral range of 290-440 nm and a spectral resolution of 0.5 FWHM. Measurements were carried out on a near horizontal scanning mode from a fixed position (Fig. 2). The SO_2 column amounts (ppm m) were retrieved from the spectra following standard procedures outlined in Platt and Stutz (2008). Reference spectra included in the non-linear fit were obtained by convolving high resolution SO_2 (Bogumil et al., 2003) and O_3 (Voigt et al., 2001) cross-sections with the instrument line shape. Fraunhofer reference and ring spectra were also included in the non linear fit. The mean total column amount of the plume cross section was then multiplied by the plume rise speed (obtained from the thermal infrared camera) to yield the SO_2 emission rate. We also deployed a miniature thermal infrared camera, the OPTRIS PI640. The camera weighs 320 g, including a lens of 62° × 49° FOV, f = 8 mm, and its dynamic range equivalent to radiant temperatures from -20 to 900 °C. The detector has 640 × 480 pixels and the operating waveband is 7.5 - 13 µm with a maximum frame rate of 80 Hz (Bani et al., 2017). The camera was positioned ~60 m to the west of the main degassing vent (Fig. 2) to capture emission dynamic.

Fresh rock samples were collected in the crater then analyzed in the laboratory using X-ray fluorescence (XRF) at BPPTKG (Balai Penyelidikan dan Pengembangan Teknologi Kebencanaan Geologi) Yogyakarta-Indonesia.

3. Results and discussions

3-1. Summit morphology: shift of active crater and mass failure

Gamkonora is a nearly perfect cone-shaped stratovolcano that culminates at 1635 m above sea level. Its western flank extends into the sea but its aerial base diameter is about 8 km. The summit crater has an elongated shape of 1500 m x 500 m, along a north-south direction (Fig. 2). The crater is widely opened to the south suggesting a crater wall failure. This latter left a void space of ~0.1 km^2. Assuming that the pre-collapse crater wall was 50 m from the rim to the floor, similar to the current situation, then one can estimate a missing volume of about 5 km^3 that may have collapsed from the summit of Gamkonora. In 1888, a similar volume (5 km^3) collapsed from Ritter Island stratovolcano (PNG) and subsequently triggered a 10-15 m height tsunami on the coasts of Bismarck Sea (Ward and Day, 2003). In contrast to the Ritter Island volcano, where the flank failure was directly into the sea, the collapse of Gamkonora was to the south, not directly towards the sea. The age of the collpase event is unkown, and more work is needed to test if a link can be established between this collapse and the 1673 Gamkonora tsunami. One alternative explaination would be a change of flow direction to the west, guided by the relief but this is yet to be confirmed.

The summit crater of Gamkonora hosts at least 3 overlapping subcraters (Fig. 2). The northermost subcrater, named crater 1 in this work, is 250 m wide and periodically hosts a lake, in particular during the wet season. In September 2018 (this work) there was no lake which allowed relatively easy access to the active crater. The biggest subcrater is situated in the central portion of the crater's terrace, is >300 m in diameter, and is referred here as crater

2. Both crater 1 and 2 are currently inactive. It is unclear which of these two is the oldest. Crater 3 in contrast has a well-preserved circular shape that cuts crater 2, suggesting a younger age (Fig. 2). With 500 m diameter at the rim and 200 m on its inner crater floor, this crater 3 constitutes the current main active site on Gamkonora and is hosting the active vent from which gas exits into the atmosphere (Fig. 3). Thermal images (Fig. 3) highlight two distinct hot features in crater 3, including the main active degassing vent to the west and a circular structure occupying the eastern part of the crater, from which steam and deluted gases are released. Given that hot surfaces are generally sustained by deep fluid circulations that carries heat to the surface (Chiodini et al., 2006), it is thus likely that this circular thermal destribution corresponds to an active, partially buried degassing structure whose role is now becoming secondary compared to the current active vent. It is also possible that the activity in crater 3 has migrated to the west, in coherence with successive changes of the Gamkonora centre of activity over time. Among the numerous reasons potentially causing volcanic activity shifts, subsurface emplacement of a cooled and dense magma (Primulyana et al., 2017), fault and fractures controls on mgma ascent (Lanzafame et al., 2003), and/or a large mass collapse that can enhance stanges in the crater, are among the most common. In any case, the elongated shape of the crater on top of Gamkonora clearly proves the progressive migration of volcanic activity, causing the successive formation of distinct craters throughout the course of its historical volcanic activity.

3-2. Basaltic andesite to andesite melt source

The bulk rock compositions obtained from fresh samples collected next to Gamkonora crater 3 are basaltic-andesitic to andesitic (Table 2, Fig. 4). Our results are derived from a limited number of samples, and can in no way be taken as representative of the entire Gamkonora eruptive activity. However, it suggests that at least the most recent activity has been sustained by a mildly evolved source magma, broadly within the typical volcanic arc range. Basaltic-andesitic to andesitic magma, expecially if erupted after relatively long repose periods of several decades (Table 1), can erupt violently into explosive eruptions. The recent Gamkonora magma composition is less differenciated than magmas currently erupted in neighboring volcanoes, Ibu and Dukono (Fig. 4), located along the same arc at respectively ~15 km and ~50 km to the northeast. Dukono magma is of andesite to trachy-andesite composition and currently feeds continuous eruptive activity (Bani et al., 2018) whilst Ibu is sustained by a dacitic source and is presently undergoing lava dome build-up associated to frequent explosive eruptions (Saing et al., 2014). Magma compositions typically evolve over time, thus it is very usual to identify distinct melt sources between neighbour volcanoes and even distinct melt compositions over the eruptive history of the same volcano. A more complete petrological/volcanological rock survey, including trace-element and isotopic analyses, is urgently needed to better characterize the Gamkonora magmatic source and its evolution over the volcano's geological hystory .

3-3. A relatively small but magmatic volatile output

Scanning DOAS measurement results are summarized in Table 3, and indicate a mean SO_2 emission rate fluctuating between 1.6 and 6.1 t/d, with a mean value of 3.4 ± 1.4 t/d. Our results thus suggest Gamkonora is currently a weak degassing source, in agreement with the small size of the plume exiting the active crater (Fig. 3). Such a small gas emission suggest "calm" quiescent activity in 2018, and is consistent with the lack of any reported eruptive activity since 2013.

In-plume gas concentrations measured with the Multi-GAS (Table 4) peaked at XXX ppmv, XXX ppmv, XXX ppmv, XXX ppmv, and XXX ppmv for H_2O, CO_2, SO_2, H_2S and H_2 respectively. The good positive correlations between the different gases recorded on Gamkonora (Fig. 5) suggest their common fumarolic source, and allow deriving the volatile ratios from the slopes of the best-fit regression lines. The derived ratios are circa 135, 5.6, 0.6, and 0.3 for H_2O/SO_2, CO_2/SO_2, H_2S/SO_2 and H_2/SO_2, respectively. The prevalence of SO_2 over H_2S, and the high equilibrium temperature of circa 670 ºC obtained by resolving together the SO_2/H_2S vs. H_2/H_2O redox equilibria (see methodology in Aiuppa et al., 2011; Moussallam et al., 2017; 2018), suggest that Gamkonora gas emissions are fed by a magmatic source with redox conditions between FeO-Fe_2O_3 and Nickel-Nickel Oxide buffers (NNO) (oxygen fugacity of 10^{-16} bars).

By converting our measured volatile ratios into molar percentages (in the assumption that no other major volcanogenic gas is present in addition to those we determined), we find that Gamkonora releases a water-rich gas, with 94.7% H_2O molar proportion, as typical for arc volcanic gases (Fischer, 2008). Our inferred concentrations for the other gases are 3.9%, 0.7%, 0.4% and 0.2% for CO_2, SO_2, H_2S and H_2 respectively. The mean CO_2/S_t ratio of 3.5 (S_t = SO_2 + H_2S) obtained for Gamkonora is above the mean arc CO_2/S_t ratio (~2) for persistently degassing open-vent arc volcanoes (Shinohara, 2013), but is well within the range of volcanic gas CO_2/S_t ratios of 3-6 in nearby Java (Aiuppa et al., 2015, 2017, 2019). Although such C-rich gas composition may be tentatively be taked to imply some substantial carbon contribution from either the slab or crustal-derived fluids (Aiuppa et al., 2017, 2019), more work is needed to fully characterize the Maluku magmatic arc gas signature and source. This is expecially true if one takes into account the CO_2-poor magmatic source observed on Dukono (Bani et al., 2018), located only ~50 km northeast of Gamkonora, which reflects the compositional heterogeneity and complex geodynamic settings of the Maluku arc.

On many volcanoes with open vents, surface degassing is the result of the sudden (periodic) release of over-pressured pockets of magmatic gases (Gaudin et al., 2017). In such situation, one can expect to observe temporal fluctuations in the gas emissions and associated heat. Figure 6 illustrates a typical temporal record of discharge temperatures at the exit of Gamkonora active vent, highlighting a continuous gas emission with an apparent low frequency (0.2-0.3 Hz) and an amplitude of 2-6 °C. Through this degassing activity, Gamkonora releases on a daily basis 129, 13, 3.4, 1.1 and 0.03 tons of H_2O, CO_2, SO_2, H_2S

and H_2 respectively (Table 3) . Such volatile output accounts for a relatively small fraction of the total volcanic gas budget in Indonesia, which includes some top-emitters such as Dukono (~820 t SO_2/d; Bani et al., 2018), Bromo (166 t SO_2/d; Aiuppa et al., 2015) or Krakatau (Bani et al., 2015).

5. Conclusions

Gamkonora is a little known but very active volcano located in North Maluku, east Indonesia. Not less than 13 eruptions have been recorded over the last 2 centuries, corresponding to about one eruption every 15 years. In many cases, these eruptions forced thousands of inhabitants to leave their villages, at least temporarily. Our results, taken during mild quiescent activity in 2018, indicate that the current Gamkonora gas emissions are dominated by water (H_2O/SO_2 ratio of 135 ± 69), and exhibit a CO_2/St mean ratio (3.5) within the compositional range for high-temperature gas emissions from other Indonesian volcanoes. This degassing activity is likely supplied by basaltic-andesitic to andesitic magma at depth. In September 2018, the volcano was emitting via main fumarolic vent a weak but persistent "magmatic" gas output, with daily fluxes of 129, 13, 3.4, 1.1 and 0.03 tons for H_2O, CO_2, SO_2, H_2S and H_2 respectively. In spite of the weak emissions measured, we argue that our results are significant for understanding the "characteristic" degassing behavior of the many A-type Indonesian volcanoes that, similarly to Gamkonora, have erupted recently, but are currently undergoing mild, closed-conduit, quiescent degassing activity. This category may include several tens of volcanoes, whose cumulative volatile output is unknown, but may make a sizable fraction of the regional volcanic degassing budget. Quantifying the gas emissions from these (yet unmeasured) volcanoes is thus central to refining estimates of the Indonesian volcanic gas budget, and to test the representatives of the Gamkonora presented here.

Acknowledgements

The research leading to these results has received support from JEAI-COMMISSION under the collaboration between CVGHM and IRD. We acknowledge the field support from Gamkonora and Ibu observatories.

References

Aiuppa, A., Shinohara, H., Tamburello, G., Giudice, G., Liuzzo, M., Moretti, R., 2011. Hydrogen in the gas plume of an open-vent volcano, Mount Etna, Italy. J. Geophys. Res. B: Solid Earth 116 (10), B10204

Aiuppa, A., Giudice, G., Liuzzo, M., Tamburello, G., Allard, P., Calabrese, S., Chaplygin, I., McGonigle, A.J.S., Taran, Y., 2012. First volatile inventory for Gorely volcano, Kamchatka. Geophys. Res. Lett. 39, L06307. http://dx.doi.org/10.1029/2012GL051177

Aiuppa, A., Bani, P., Moussallam, Y., DiNapoli, R., Allard, P., Gunawan, H., Hendrasto, M., Tamburello, G., 2015. First determination of magma-derived gas emissions from Bromo

volcano, eastern Java (Indonesia). J. Volcanol. Geotherm. Res. vol.304, p.206-213, DOI:10.1016/j.jvolgeores.2015.09.008

Aiuppa, A., Fischer, T. P., Plank, T., Robidoux, P., Di Napoli, R. (2017). Along-arc and inter-arc variations in volcanic gas CO2/ST ratios reveal dual source of carbon in arc volcanism. Earth-Science Reviews, 168, pp. 24–47

Aiuppa, A., Fischer, T. P., Plank, T., & Bani, P. (2019). CO2 flux emissions from the Earth's most actively degassing volcanoes, 2005–2015. Scientific Reports, 9 (5442).

Bani, P., Normier, A., Bacri, C., Allard, P., Gunawan, H., Hendrasto, M., Surono, Tsanev, V., 2015. First measurement of the volcanic gas output from Anak Krakatau, Indonesia. J. Volcanol. Geotherm. Res. vol.302, p.237-241, DOI:10.1016/j.jvolgeores.2015.07.008

Bani, P., Alfianti, H., Aiuppa, A., Oppenheimer, C., Sitinjak, P., Tsanev, V., Saing, U.B., 2017. First study of heat and gas budget for Sirung volcano, Indonesia. Bulletin of Volcanology 79(8):60. https://doi.org/10.1007/s00445-017-1142-8

Bani, P., Tamburello, G., Rose-Koga, E., Liuzzo, M., Aiuppa, A., Cluzel, N., Amat, I., Syahbana, D.K., Gunawan, H., Bitetto, M., 2018. Dukono, the predominant source of volcanic degassing in Indonesia, sustained by a depleted Indian-MORB. Bulletin of Volcanology 80, 5, DOI:10.1007/s00445-017-1178-9

Bogumil, K., Orphal, J., Homann, T., Voigt, S., Spietz, P., Fleischmann, O.C., Vogel, A., Harmann, M., Kromminga, H., Bovensmann, H., Frerick, J., Burrows, J.P., 2003. Measurements of molecular absorption spectra with SCIAMACHY preflight model: instrument characterization and reference data for atmospheric remote sensing in the 230-2380 nm region. J. Photochem. Photobiol. A. 157(2-3):167-184. https://doi.org/10.1016/S1010-6030(03)00062-5

Buck, A. L., 1981. New equations for computing vapor pressure and enhancement factor. Journal of Applied Meteorology 20.12, pp. 1527-1532. doi: 10.1175/1520-0450(1981)020<1527:nefcvp>2.0.co;2

Data Dasar Gunungapi Indonesia, 2011. Kementerian Energi dan Sumber daya Mineral, Badan Geologi. edisi kedua, 401-410

Fischer, T.P., 2008. Fluxes of volatiles (H_2O, CO_2, N_2, Cl, F) from arc volcanoes. Geochem. J., 42, 21-38

Gaudin, D., Taddeucci, J., Scarlato, P., Harris, A., Bombrun, M., Del Bello, E., Ricci, T., 2017. Characteristics of puffing activity revealed by ground-based, thermal infrared imaging: the example of Stromboli Volcano (Italy). Bulletin of Volcanology 79:24, doi:10.1007/s00445-017-1108-x

Global Volcanism Program, 1981. Report on Gamkonora (Indonesia). In: McClelland, L (ed.), Scientific Event Alert Network Bulletin, 6:7. Smithsonian Institution https://doi.org/10.5479/si.GVP.SEAN198107-268040

Global Volcanism Program, 2013. Gamkonora (268040), in Volcanoes of the World, v. 4.8.2. Venzke, E. (ed.). Smithsonian Institution https://doi.org/10.5479/si.GVP.VOTW4-2013

Kusumadinata, K., 1969. Kumpulan data mengenai Gunung Gamkonora di Pulau Halmahera (Maluku Utara), Direktorat Vulkanologi, 58 pp.

Lanzafame, G., Neri, M., Acocella, V., Billi, A., Funiciello, R., Giordano, G., 2003. Structural features of the July-August 2001 Mount Etna eruption: evidence for a complex magma supply system. J. Geological Society, 160, 531-544

Moussallam, Y., Peters, N., Masias, P., Aaza, F., Barnie, T., Schipper, C.I., Curtis, A., Tamburello, G., Aiuppa, A., Bani, P., Giudice, G., Pieri, D., Davies, A.G., Oppenheimer, C., 2017. Magmatic gas percolation through the old lava dome of El Misti volcano. Bull. Volcanol. 79:46, doi: 10.1007/s00445-017-1129-5

Moussallam, Y., Bani, P., Schipper, C.I., Cardona, C., Franco, L., Barnie, T., Amigo, A., Curtis, A., Peters, N., Aiuppa, A., Giudice, G., Oppenheimer, C., 2018. Unrest at the Nevados de Chillán volcanic complex: a failed or yet to unfold magmatic eruption? Volcanica 1(1): 19-32. doi: 10.30909/vol.01.01.1932

Paris, R., Switzer, A.D., Belousova, M., Belousov, A., Ontowirjo, B., Whelley, P.L., Ulvrova, M., 2014. Volcanic tsunami: a review of source mechanisms, past events and hazards in Southeast Asia (Indonesia, Philippines, Papua New Guinea). Nat Hazards 70:447–470

DOI 10.1007/s11069-013-0822-8

Platt, U., Stutz, J., 2008. Differential optical absorption spectroscopy, Principles and Applications. Springer, 597 pp

Primulyana, S., Bani, P., Harris, A., 2017. The effusive-explosive transitions at Rokatenda 2012-2013: unloading by extrusion of degassed magma with lateral gas flow. Bull. Volcanol. 79: 22, doi:10.1007/s00445-017-1104-1

Saing, U.B., Bani, P., Kristianto, 2014. Ibu volcano, a center of spectacular dacite dome growth and long-term continuous eruptive discharges. J. Volcanol. Geotherm. Res. 282:36-42. https://doi.org/10.1016/j.jvolgeores.2014.06.011

Shinohara, H., 2013. Volatile flux from subduction zone volcanoes: insights from a detailed evaluation of the fluxes from volcanoes in Japan. J. Volcanol. Geotherm. Res. 268, 46-63

Siebert, L., Simkin, T., Kimberly, P., 2010. Volcanoes of the world, 3rd edition, Smithsonian Institution

Suparman Y., et al., 2013. Laporan Tanggap Darurat Gunungapi Gamkonora, Maluku Utara. Pusat Vulkanologi dan Mitigasi Bencana Geologi, p. 7

Tamburello, G., 2015. Ratiocalc: Software for processing data from multicomponent volcanic gas analyzers. Computers & Geosciences 82, pp. 63–67. doi:10.1016/j.cageo.2015.05.004

Voigt, S., Orphal, J., Bogumil, K., Burrows, J.P., 2001. The temperature dependence (203–293 K) of the absorption cross-sections of O_3 in the 230–850 nm region measured by Fourier-transform spectroscopy. J. Photochem. Photobiol. A. 143(1):1-9. https://doi.org/10.1016/S1010-6030(01)00480-4

Ward, S.N. & Day, S., 2003. Ritter Island volcano - lateral collapse and the tsunami of 1888.Geophys. J. Int.154, 891-902

Captions

Table 1. Eruptive history of Gamkonora volcano

Date	Eruptive event
1564 or 1565	Strong eruption (VEI 3) at the summit crater. The blast was heard up to 200 km from the volcano. Lava flow reached the sea and heavy ash fall have caused significant damage to the forests and cultivated land. The eruption have caused human losts but no further information are available. Kusumadinata (1969), Data dasar (2011), GVP (2013) and Siebert et al. (2010)
1673 (May 20)	Large and massive eruption (VEI 5) have triggered a tsunami that inundated the surrounding coastal villages. The eruption was accompanied by felt earthquakes. Ash dispersal have cause pitch-dark on Ternate city. Heavy ash fall reported on Manado, Sangir Islands (North Sulawesi) and even on Mindanao (southern Philippines). Forests and agricultural surfaces were extensively devastated. The dead toll related to the eruption is unknown but likely significant. Kusumadinata (1969), Data dasar (2011), GVP (2013) and Siebert et al. (2010)
1774 (Oct. 8)	Eruption at Gamkonora but no further information. Kusumadinata (1969)
1890	Eruption column above Gamkonora was visible from Ternate (VEI 2). Kusumadinata (1969) and GVP (2013)
1917 (Oct. 18)	Eruption that built a thick column (VEI 2) with lightnings. Kusumadinata (1969), Data dasar (2011) and GVP (2013)
1926 (Jun. 1-2)	Explosive eruption from the central crater developing a thick plume above the crater. Incandescent light were seen at night (VEI 1). Kusumadinata (1969), Data dasar (2011) and GVP (2013)
1949	Explosive eruption (VEI 2) leading ash fall around the crater. Kusumadinata (1969), Data dasar (2011) and GVP (2013)
1950 (Oct.)	Eruption at the summit have enduced forest fire around the south-southwest crater rim (VEI 2). Thick ash was observed. Kusumadinata (1969), Data dasar (2011) and GVP (2013)
1951 (Apr. 12)	Eruption sending a black plume into the atmosphere (VEI 2). Plume puff was observed from Gamsungi village. Data dasar (2011) and GVP (2013)
1952 (Jul. 16, Aug. 25, 31)	Eruption (VEI 2) developping a black column up to 1 km above the crater. Kusumadinata (1969) and GVP (2013)
1981 (Mar.-Jul.)	Eruption (VEI 1) with ash plume reaching 700 m and ash fall up to 5 km distance from the volcano. Incandescent products were seen projected above the summit. Over 3500 inhabitants fled their villages. GVP (2013) and https://www.volcanodiscovery.com/gamkonora.html
1983 (Feb. 16-17)	Ash eruption occurred but no further information. Data dasar (2011)
1987 (Apr. 13-26)	Minor ash eruptions (VEI 1) with plume reaching 700 m height. Minor ashfall on the flanks. Some coastal residents went to evacuate themselves. Data dasar (2011) and GVP (2013)
1997 (Jan. 10)	Minor ash eruption with plume reaching 200 m height above the summit (VEI 1). Data dasar (2011)

2007 (Jul. 8-11)	Eruption that commenced with a phreatic eruption then progressively became magmatic with ash plume reaching 4000 m above the summit (VEI 2). Incandescent products were propelled 5-50 m above the crater and intermittently showered the flank. About 8,400 people were evacuated from their villages situated within 8 km radius from the volcano. GVP (2013) and Data dasar (2011)
2012 (Jun. 13)	Explosive eruption occurred in the main crater (VEI 2), plumes rose to 3000 m above the summit and ash spread out to the northeast. GVP (2013) and Suparman (2013)
2013 (Jan. 24)	Eruption in the main crater (VEI 2) produced a thick gray ash plume column reached up to 2000-2500 m above the summit. Suparman (2013)

Table 2. Melt composition of Gamkonora volcano

Oxides	Rock sample 1	Rock sample 2
SiO_2 (wt %)	55.86	58.47
Al_2O_3 (wt %)	16.96	17.05
Fe_2O_3 (wt %)	9.39	8.57
CaO (wt %)	7.09	6.73
MgO (wt %)	3.36	2.74
Na_2O (wt %)	3.78	4.02
K_2O (wt %)	1.36	1.55
TiO_2 (wt %)	0.85	0.80
MnO (wt %)	0.18	0.16
P_2O_5 (wt %)	0.21	0.24

Table 3. SO_2 flux result from DOAS scanning measurements

Scan N°	Start Time (UT)	End Time (UT)	Step angle (°)	Number of spectra	Average C.A. (g/cm^2)	SO_2 Flux	
						kg/s	t/d
1	03:37	03:41	10.0	14	0.10	0.01	1.6 ± 0.8
2	03:41	03:43	10.0	14	0.19	0.04	3.9 ± 1.1
*3**	*03:46*	*03:49*	*5.4*	*24*	*0.05*	*0.01*	*1.1 ± 1.0*
*4**	*03:49*	*03:52*	*5.4*	*24*	*0.04*	*0.01*	*0.6 ± 0.5*
5	03:53	03:57	5.4	24	0.21	0.07	6.1 ± 1.4
6	03:58	04:01	5.4	24	0.07	0.03	2.6 ± 1.7
7	04:02	04:05	5.4	24	0.08	0.04	3.7 ± 2.2
*8**	*05:03*	*05:04*	*5.4*	*24*	*0.03*	*0.01*	*0.7 ± 1.2*
9	05:06	05:09	5.4	24	0.08	0.03	2.3 ± 1.4
*10**	*05:09*	*05:12*	*5.4*	*24*	*0.03*	*0.01*	*0.8 ± 1.8*
11	*05:13*	*05:15*	*5.4*	*24*	*0.06*	*0.01*	*0.8 ± 0.7*
						Mean SO_2 flux = 3.4 ± 1.4 t/d	

** Scans not included in the mean SO_2 flux given the high error induced by plume direction change.*

Table 4. Gamkonora in-plume gas concentrations, gas ratios and fluxes

Gas concentrations		
Mean H_2O (ppm v)	951 ± 177	
Mean CO_2 (ppm v)	403 ± 8	
Mean SO_2 (ppm v)	0.6 ± 0.1	
Mean H_2S (ppm v)	0.4 ± 0.01	
Mean H_2 (ppm v)	3.2 ± 0.4	
Gas Ratios		
H_2O/SO_2	135 ± 69	
CO_2/SO_2	5.6 ± 1.3	
H_2S/SO_2	0.6 ± 0.03	
H_2/SO_2	0.3 ± 0.1	
Gas composition and flux estimates		
	Composition (mol %)	**Flux (t/d)**
H_2O	94.7	129 ± 53
CO_2	3.9	13 ± 5
SO_2	0.7	3.4 ± 1.4
H_2S	0.4	1.1 ± 0.4
H_2	0.2	0.03 ± 0.01

Figure 1. Gamkonora is one of the active volcano of Halmahera arc and is one of the 3 active volcanoes of Halmahea Island, North Maluku.

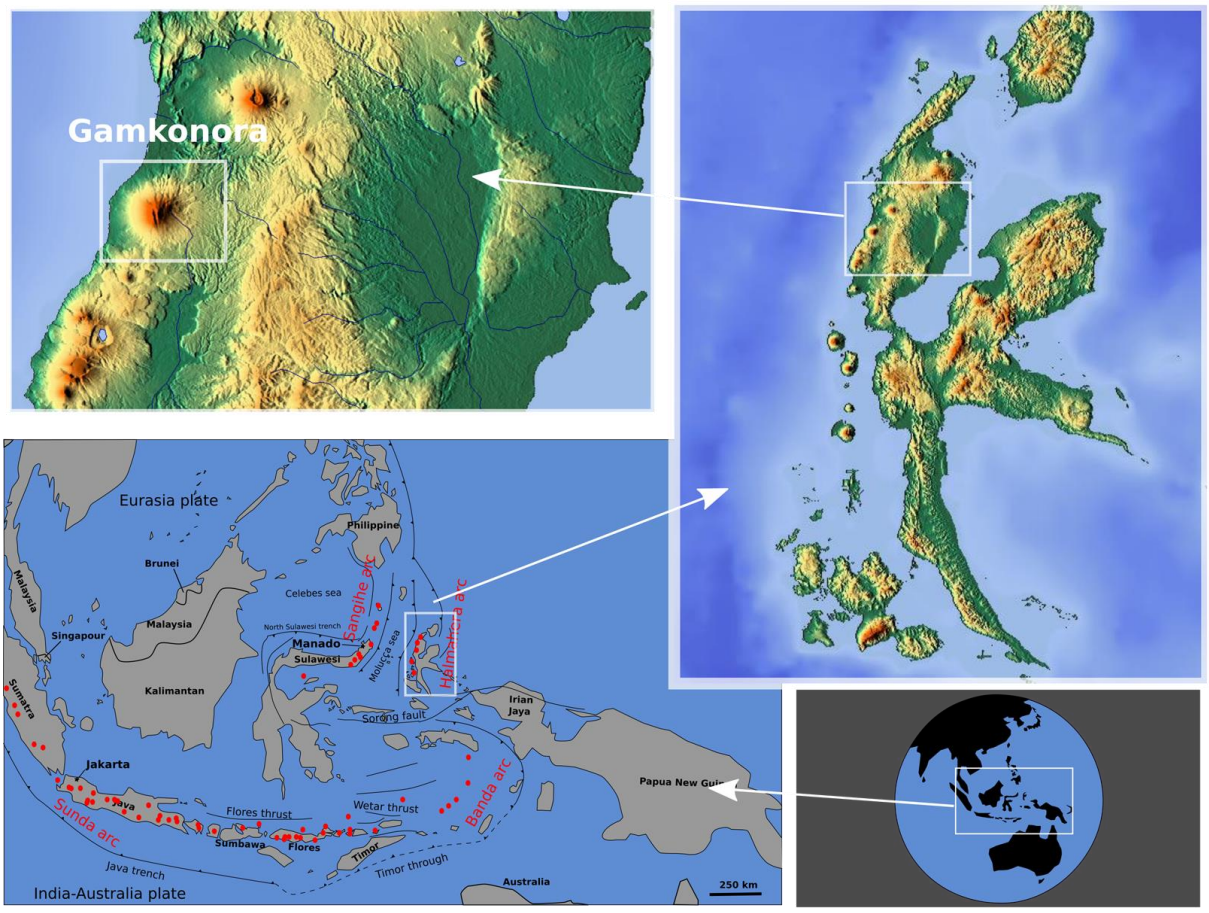

Figure 2. Gamkonora is a large volcano that extends into the sea (A). Its summit hosts an elongated crater (B) formed by successive emplacement of crater 1, crater 2 and crater 3 (C). Crater 1 periodically hosts a lake. Crater 3 is the current active crater.

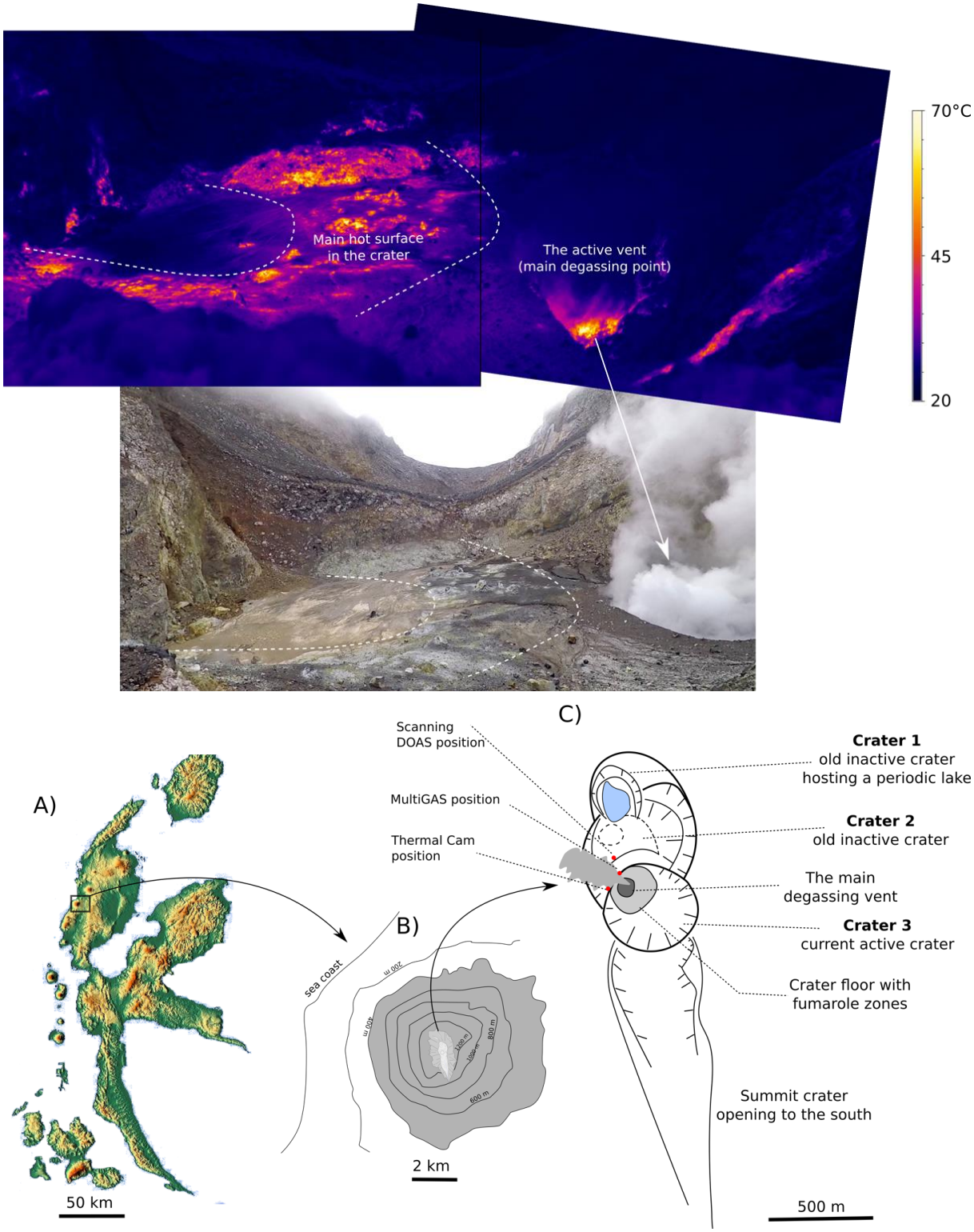
70°C
45
20
Main hot surface
in the crater
The active vent
(main degassing point)
A)
50 km
B)
sea coast
200 m
400 m
600 m
800 m
1000 m
1200 m
2 km
C)
Scanning
DOAS position
MultiGAS position
Thermal Cam
position
Crater 1
old inactive crater
hosting a periodic lake
Crater 2
old inactive crater
The main
degassing vent
Crater 3
current active crater
Crater floor with
fumarole zones
Summit crater
opening to the south
500 m

Figure 3. Detailed view of the active crater 3. Thermal images highlight two distinct hot surfaces, including the active vent and a circular hot structure.

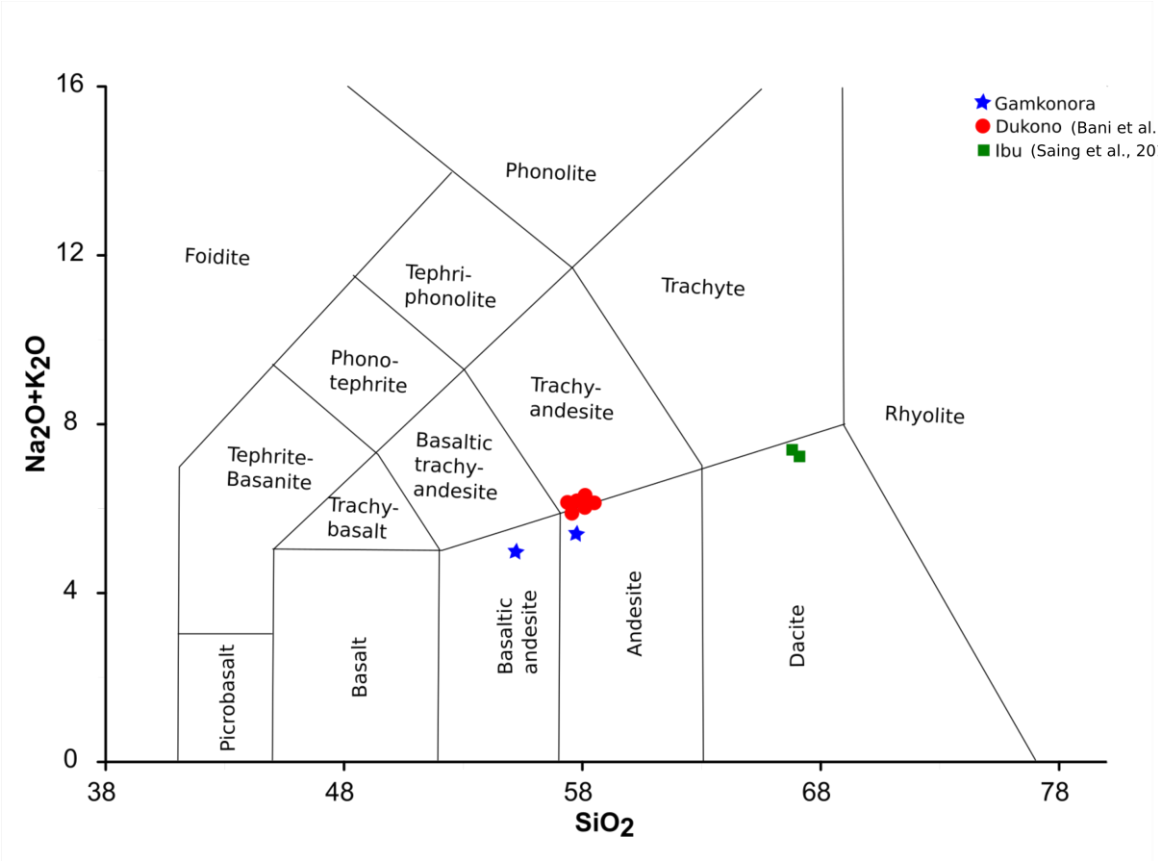

Figure 4. Basaltic andesite to andesite melt composition that sustained the current Gamkonora activity. Dukono and Ibu melt source are also plotted for comparison. These latters are more defferentiated.

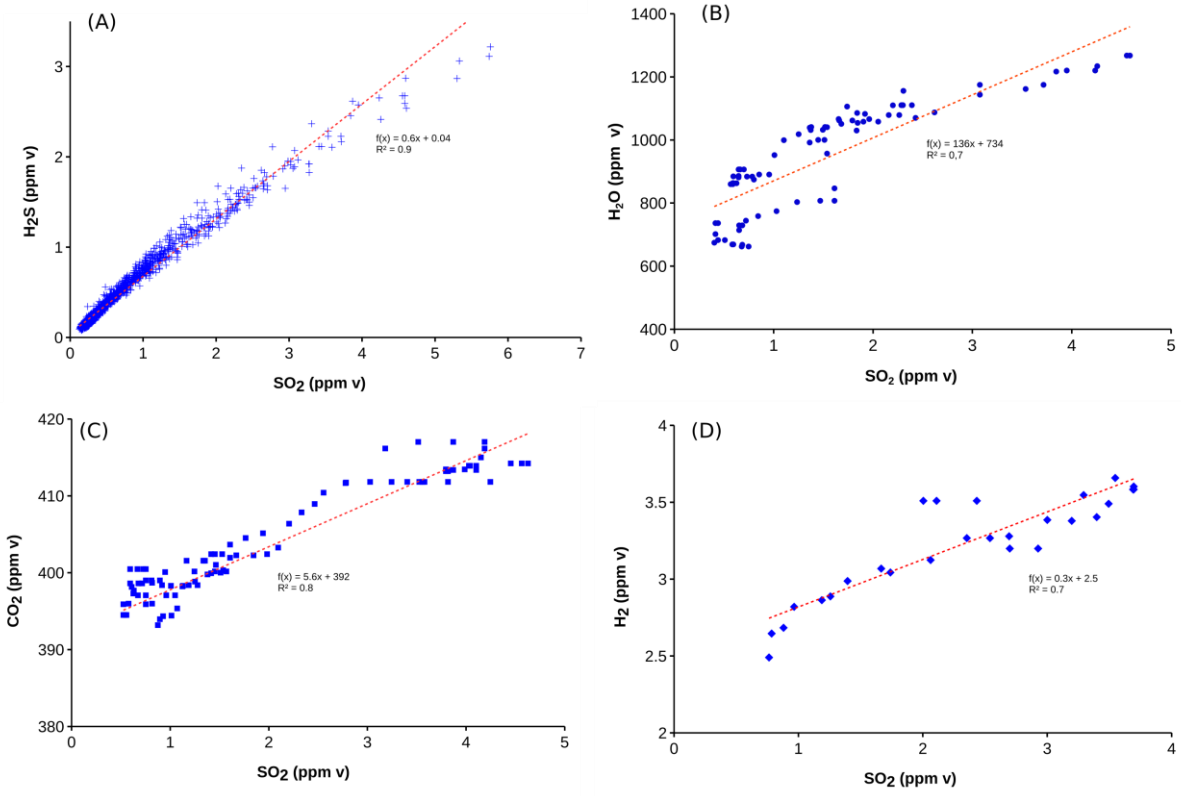

Figure 5. Typical gas/SO_2 correlation obtained on Gamkonora.

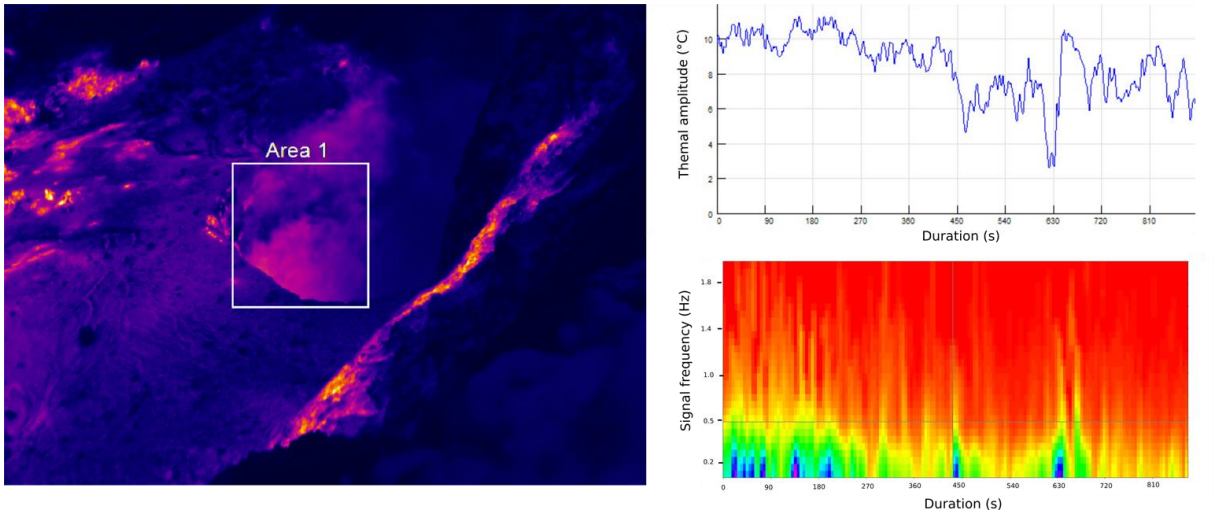

Figure 6. Temperature fluctuation induce by hot gases that exit the active vent. The white scare (left, Area 1) is the zone of interest on which the mean temperature is recorded. The temperature amplitude (top right) and the spectrogram (bottom right) denote the dynamic of degassing on Gamkonora.